

Fermion perturbations in string-theory black holes

Owen Pavel Fernández Piedra*

¹ *Instituto de Física, Universidade de São Paulo,
CP 66318, 05315-970, São Paulo, Brazil , and*

² *Departamento de Física y Química,
Universidad de Cienfuegos, Carretera a Rodas,
Cuatro Caminos, s/n. Cienfuegos, Cuba*

Jeferson de Oliveira†

*Instituto de Física, Universidade de São Paulo,
CP 66318, 05315-970, São Paulo, Brazil*

(Dated: August 30, 2021)

Abstract

In this paper we study fermion perturbations in four dimensional black holes of string theory, obtained either from a non-extreme configuration of three intersecting five-branes with a boost along the common string or from a non-extreme intersecting system of two two-branes and two five-branes. The Dirac equation for the massless neutrino field, after conformal re-scaling of the metric, is written as a wave equation suitable to study the time evolution of the perturbation. With the aid of Prony fitting of time-domain profile we calculate the complex frequencies that dominate the quasinormal ringing stage, and also determine this quantities by the semi-analytical sixth order WKB method. We also find numerically the decay factor of fermion fields at very late times, and show that the falloff is identical to those appeared for massless fields in other four dimensional black hole spacetimes.

PACS numbers: 02.30Gp, 03.65ge

* opavel@ucf.edu.cu

† jeferson@fma.if.usp.br

I. INTRODUCTION

String theory and its generalization in terms of extended objects named M/Dp-branes is a promising candidate for a fundamental quantum theory of all interactions [1], including a description of black holes in a quantum gravity framework [2].

The scenario of string theory is consistently formulated only in higher dimensions, which are usually compactified, so a full description of a black hole whose event horizon is comparable to the size of extra dimensions has to be in terms of such higher dimensional description. So, in order to discuss the production of small black holes in the Large Hadron Collider (LHC) and the evaporation of black holes by Hawking effect, we must consider solutions coming from a string theory/branes picture.

One class of solutions which encompass the features of string theory and also can be interpreted as black holes are those non-extremal solutions which came from intersections of branes in string theory or in M-theory [3][4][5][6]. The parameters of such black holes can be deduced by corresponding compactifications of the higher dimensions.

In this work we aim at studying the question of stability of a family of four-dimensional black holes in string theory. In order to perform this we calculate the quasinormal spectrum due to a perturbation of a Dirac field evolving in the background given by the stringy black hole. Regarding the stability of extended objects from low energy limit of string theory, some work has been done [7], where it was considered a probe scalar field evolving in a p -brane geometry and its quasinormal spectrum in order to analyze the stability and the relation between the parameters of p -brane and the quasinormal ringing.

Quasinormal modes (QNM) of black holes has been extensively studied since the pioneering work on stability of Schwarzschild singularity performed by Regge and Wheeler [8]. In studying quasinormal spectrum, we can gain some valuable information about the parameters which characterize the solution, because there are definite relations between the QNM and the parameters of solution, see [9] and references therein. Such QNM are characterized by a well-defined set of complex frequencies and encode the response of black hole to external perturbation, so we can study the stability of a black hole against small perturbations due to probe fields or the geometry itself through its quasinormal spectrum.

Besides, further developments in QNM research in the context of AdS/CFT and holography allow us to calculate the location of the poles of the retarded correlators functions of

certain gauge theories [10] and reveals some connection between the dynamics of black hole horizons and the hydrodynamics [11] [12].

The paper is organized as follows: Section II gives a review about the casual structure of four dimensional black hole obtained from intersections of branes. In Section III we obtain the wave equation suitable to analyze the propagation of a Dirac field in the background geometry of the four dimensional stringy black hole. Section IV is devoted to numerically solve the evolution equation of such fields in the considered background, and in Section V we will be concerned with the quasinormal stage, and compute the complex quasinormal frequencies using two methods: Prony fitting of time domain data and the sixth order WKB approach. The results of a numerical investigation of the relaxation of Dirac perturbations in stringy black holes at very long times are presented in Section VI. In Section VII we present an analytical expression for the quasinormal frequencies in the limit of large angular momentum, followed by the last section of the paper, which contains some concluding remarks of our work.

II. (3+1)-DIMENSIONAL BLACK HOLE SOLUTION FROM INTERSECTING BRANES

The metric of the non-extremal 4-dimensional black hole obtained from intersections of five-branes read as [4]

$$ds^2 = f^{-1/2} \left(1 - \frac{r_H}{r}\right) dt^2 + f^{1/2} \left[\left(1 - \frac{r_H}{r}\right)^{-1} dr^2 + r^2 d\Omega_2^2 \right], \quad (1)$$

where

$$f = \left(1 + \frac{r_H Q_1}{r}\right) \left(1 + \frac{r_H Q_2}{r}\right) \left(1 + \frac{r_H Q_3}{r}\right) \left(1 + \frac{r_H Q_4}{r}\right). \quad (2)$$

This metric represents a family of black hole solutions parametrized by r_H , which gives the location of the event horizon, and four charges Q_1, Q_2, Q_3, Q_4 given by :

$$Q_i = \sinh^2(\delta_i), \quad i = 1, 2, 3, 4$$

that are written in terms of five-brane parameters δ_i , resulting from the compactification of higher dimensions. This solution describes a four dimensional Schwarzschild black hole in the case which the charges Q_i are all zero. Also the metric is asymptotically flat and, as we

shall see below, has a regular event horizon located at $r = r_H$ even with all charges different from zero. Besides, the redshift goes to infinity in such surface.

Infinity redshift surfaces can be found, for a given metric, through the following relation

$$\nu = \nu_0 \sqrt{\frac{g_{00}(x_{source}^a)}{g_{00}(x^a)}}, \quad (3)$$

which relates the frequency ν measured by an observer at rest away from the source, whose emission frequency of say, light pulses, is ν_0 .

In order to have a infinity redshift surface, the frequency ν has to be zero, it means the frequency ν was infinitely delayed due to gravitational effects. So, equation(3) implies

$$g_{00}(x_{source}^a) = 0, \quad (4)$$

given us the location of the infinity redshift surfaces. In the case of the spacetime of four dimensional stringy black holes (1) it is easy to see that $r = r_H$ and $r = 0$ are the surfaces where the redshift of in-falling objects goes to infinity.

As in Schwarzschild solution, such surface $r = r_H$ acts as a one-way membrane for physical objects whose trajectories lie in or on the forward light cone. To see this, suppose a smooth hypersurface S defined by the equation

$$u(x^a) = const.$$

The vector $N_a = \partial_a u$ is normal to S , so if S is a one-way membrane it has to be a null hypersurface, therefore the norm of N_a has to be null as well. So,

$$g^{ab} N_a N_b = 0,$$

determine the one-way membranes, which in our case are located at $r = r_H$ and $r = 0$. However, for the one of the four charges Q_i equal to zero, only $r = r_H$ is a null and infinity redshift hypersurface, $r = 0$ is a genuine space-time singularity, as we will see below in more detail.

Let us consider the Kretschmann invariant for the spacetime (1), where we take for simplicity $Q_i = q$ (the result holds as well for four different charges):

$$R^{abcd} R_{abcd} = \frac{4}{(r_H q + r)^8} P(r), \quad (5)$$

where

$$P(r) = r_H^4 q^2 (5 + 4q + q^2) - 2r_H^3 q r (3 + 7q + 2q^2) + (r_H r)^2 (3 + 8q + 8q^2) - 2r_H r^3 + r^4.$$

As we see from the above expressions, for $r \rightarrow r_H$ we have

$$R^{abcd} R_{abcd}(r \rightarrow r_H) \rightarrow \text{const},$$

and for $r \rightarrow 0$

$$R^{abcd} R_{abcd}(r \rightarrow 0) \rightarrow \frac{4}{r_H^8 q^8} [r_H^4 q^2 (5 + 4q + q^2)]. \quad (6)$$

We see clearly that $r = 0$ is not a spacetime singularity but, as previously pointed out by Horowitz *et al* [13] it is actually a inner horizon. However, if at least one of the charges is zero, the surface $r = 0$ becomes singular as we see explicitly in the expression (6).

We conclude that for at least one charge Q_i zero, we have a four dimensional black hole with a spacetime singularity located at $r = 0$ covered by a event horizon at $r = r_H$ which is also a infinity redshift surface, as expected for a spherically symmetric space time. On the other hand, if all charges are non-zero, we have a regular black hole with a event horizon at $r = r_H$ and a inner horizon at $r = 0$.

III. FUNDAMENTAL EQUATIONS

In curved space-time the massless Dirac equation is written as

$$\nabla \Psi = 0, \quad (7)$$

where $\nabla = \Gamma^\mu \nabla_\mu$ is the Dirac operator that acts on the four-spinor Ψ , Γ_μ are the curved space Gamma matrices, and the covariant derivative is defined as $\nabla_\mu = \partial_\mu - \frac{1}{4} \omega_\mu^{ab} \gamma_a \gamma_b$, with μ and a being tangent and space-time indices respectively, related by the basis of orthonormal one forms $\vec{e}^a \equiv e_\mu^a$. The associated connection one-forms $\omega_\mu^{ab} \equiv \omega^{ab}$ obey $d\vec{e}^a + \omega^a_b \wedge \vec{e}^b = 0$, and the γ^a are flat space-time gamma matrices related with curved-space ones by $\Gamma^\mu = e^\mu_a \gamma^a$. They form a Clifford algebra in d dimensions, i e, they satisfy the anti-commutation relations $\{\gamma^a, \gamma^b\} = -2\eta^{ab}$, with $\eta^{00} = -1$.

First consider some properties of the Dirac operator that will be used in future calculations [14, 15]. Under a conformal transformation of the metric of the form :

$$g_{\mu\nu} = \Omega^2 \tilde{g}_{\mu\nu}, \quad (8)$$

the spinor ψ and the Dirac operator transforms as

$$\psi = \Omega^{-\frac{3}{2}} \tilde{\psi}, \quad (9)$$

$$\nabla\psi = \Omega^{-\frac{5}{2}} \tilde{\nabla}\tilde{\psi}. \quad (10)$$

If the line element of a space-time metric takes the form of a sum of independent components $ds^2 = ds_1^2 + ds_2^2$, where $ds_1^2 = g_{ab}(x)dx^a dx^b$ and $ds_2^2 = g_{mn}(y)dy^m dy^n$ then Dirac operator ∇ satisfies a direct sum decomposition

$$\nabla = \nabla_x + \nabla_y. \quad (11)$$

The above mentioned properties of spinors and the Dirac operator in direct sum metrics and conformal related ones, allows a simple treatment of the massless Dirac equations in curved spacetimes. For two conformally related metrics, the validity of massless Dirac equation in one implies the the validity of the same equation in the other. Then, the idea is to solve the Dirac equation in the curved space described by an initial metric tensor performing successive conformal transformations that isolate the metric components that depend of a given variable, and applied successively the direct sum decomposition of Dirac operator, until to obtain an equivalent problem in a spacetime of the form $M^2 \times \sum^2$, where M^2 is two-dimensional Minkowski spacetime and \sum^2 is a two-dimensional maximally symmetric one, in which the spectrum of massless Dirac operator is known.

The method work as follows. First, in the following we suppose that our four dimensional metric is spherically symmetric, and given by:

$$ds^2 = g_{\mu\nu} dx^\mu dx^\nu = -A(r)dt^2 + B(r)dr^2 + C(r)d\Omega_2^2, \quad (12)$$

where $d\Omega_2^2$ denotes the metric for the (2)-sphere S^2 .

It is easy to show that with the identification $(t, r, \theta, \phi) \rightarrow (0, 1, 2, 3)$ if we choose the basis one-forms as $\vec{e}^0 = \vec{e}^0(t, r) = f_{(t)}(t, r)dt + f_{(r)}(t, r)dr$, $\vec{e}^1 = \vec{e}^1(t, r) = g_{(t)}(t, r)dt + g_{(r)}(t, r)dr$ and $\vec{e}^k = \vec{e}^k(\theta, \phi) = h_{(\theta)}^{(k)}(\theta, \phi)d\theta + h_{(\phi)}^{(k)}(\theta, \phi)d\phi$, $k = 2, 3$ then we have some conection one-forms that are equal to zero, and only $\omega_0^0, \omega_1^0, \omega_0^1, \omega_1^1$ and $\omega^i_j; i, j = 2, 3$ are different from

zero. This fact allows us to write $\nabla_a = \nabla_a \mathbf{I}_{(2)}$; $a = 0..3$, where $\mathbf{I}_{(2)}$ is the unit matrix in two dimensions [16].

Now, under a conformal rescaling of the form $ds^2 = C(r)d\tilde{s}^2$, where:

$$d\tilde{s}^2 = -\frac{A}{C}dt^2 + \frac{B}{C}dr^2 + d\Omega_2^2, \quad (13)$$

we need to solve the equation $\tilde{\nabla}\tilde{\psi} = \tilde{\Gamma}^\mu\tilde{\nabla}_\mu\tilde{\psi} = 0$, with $\tilde{\psi} = C^{\frac{3}{2}}\psi$. In general, the Dirac matrices $\tilde{\Gamma}^\mu$ can be chosen as:

$$\tilde{\Gamma}^0 = \tilde{\Gamma}_{(2)}^0 \otimes \mathbf{I}_{(2)}, \quad (14)$$

$$\tilde{\Gamma}^1 = \tilde{\Gamma}_{(2)}^1 \otimes \mathbf{I}_{(2)}, \quad (15)$$

$$\tilde{\Gamma}^2 = \tilde{\Gamma}_{(2)}^5 \otimes \tilde{\Gamma}_{(2)}^0, \quad (16)$$

$$\tilde{\Gamma}^3 = \tilde{\Gamma}_{(2)}^5 \otimes \tilde{\Gamma}_{(2)}^1, \quad (17)$$

where $\tilde{\Gamma}_{(2)}^0$, $\tilde{\Gamma}_{(2)}^1$ and $\tilde{\Gamma}_{(2)}^5 = -\tilde{\Gamma}_{(2)}^0\tilde{\Gamma}_{(2)}^1$ are two-dimensional Gamma matrices, and $(\tilde{\Gamma}_{(2)}^5)^2 = \mathbf{I}_{(2)}$.

Since the orbit-space part and the angular part of the metric are completely separated, one can write the Dirac equation in the form:

$$\left[\left(\tilde{\Gamma}_{(2)}^0 \tilde{\nabla}_0 + \tilde{\Gamma}_{(2)}^1 \tilde{\nabla}_1 \right) \otimes \mathbf{I}_{(2)} + \tilde{\Gamma}_{(2)}^5 \otimes \left(\tilde{\Gamma}^a \tilde{\nabla}_a \right)_{S_2} \right] \tilde{\psi} = 0, \quad (18)$$

where $\left(\tilde{\Gamma}^a \tilde{\nabla}_a \right)_{S_2}$ denotes the Dirac operator in the 2-sphere, whose orthogonal set of eigen-spinors $\tilde{\xi}_\ell^{(\pm)}$ are defined by [17]:

$$\left(\tilde{\Gamma}^a \tilde{\nabla}_a \right)_{S_2} \tilde{\xi}_\ell^{(\pm)} = \pm i(\ell + 1) \tilde{\xi}_\ell^{(\pm)}, \quad (19)$$

where $l = 0, 1, 2, \dots$. Now expanding $\tilde{\psi}$ as:

$$\tilde{\psi} = \sum_\ell \left(\tilde{\varphi}_\ell^{(+)} \tilde{\xi}_\ell^{(+)} + \tilde{\varphi}_\ell^{(-)} \tilde{\xi}_\ell^{(-)} \right). \quad (20)$$

we can put the Dirac equation in the form:

$$\left\{ \tilde{\Gamma}_{(2)}^0 \tilde{\nabla}_0 + \tilde{\Gamma}_{(2)}^1 \tilde{\nabla}_1 + \tilde{\Gamma}_{(2)}^5 [\pm i(\ell + 1)] \right\} \tilde{\varphi}_\ell^{(\pm)} = 0, \quad (21)$$

In the following we shall work with the + sign solution, because the - sign case can be worked in the same form. Denoting as $\tilde{ds}_1^2 = -\frac{A}{C}dt^2 + \frac{B}{C}dr^2$ the $t - r$ part of the metric (13) and doing a conformal rescaling of it in the form:

$$d\tilde{s}_1^2 = \frac{A}{C} [-dt^2 + dr_*^2], \quad (22)$$

where $dr_* = \sqrt{\frac{B}{A}} dr$ is the tortoise coordinate, we have:

$$\left[\gamma^t \partial_t + \gamma^{r_*} \partial_{r_*} + i\gamma^5 \sqrt{\frac{A}{C}} (\ell + 1) \right] \tilde{\varphi}_\ell^{(+)} = 0, \quad (23)$$

being γ^t and γ^{r_*} Dirac matrices in the two-dimensional Minkowski space-time with metric $ds^2 = -dt^2 + dr_*^2$.

Now choosing the representation of Dirac matrices given by:

$$\gamma^t = -i\sigma^3, \quad \gamma^{r_*} = \sigma^2, \quad \gamma^5 = (-i\sigma^3)(\sigma^2) = -\sigma^1, \quad (24)$$

where the σ^i are the Pauli matrices:

$$\sigma^1 = \begin{pmatrix} 0 & 1 \\ 1 & 0 \end{pmatrix}, \quad \sigma^2 = \begin{pmatrix} 0 & -i \\ i & 0 \end{pmatrix}, \quad \sigma^3 = \begin{pmatrix} 1 & 0 \\ 0 & -1 \end{pmatrix}, \quad (25)$$

and writing

$$\tilde{\varphi}_\ell^{(+)} = \begin{pmatrix} i\zeta_\ell(t, r) \\ \chi_\ell(t, r) \end{pmatrix}, \quad (26)$$

we obtain the following equations for each component of the Dirac spinor $\tilde{\varphi}_\ell$:

$$i \frac{\partial \zeta_\ell}{\partial t} + \frac{\partial \chi_\ell}{\partial r_*} + \Lambda_\ell \chi_\ell = 0, \quad (27)$$

and

$$i \frac{\partial \chi_\ell}{\partial t} - \frac{\partial \zeta_\ell}{\partial r_*} + \Lambda_\ell \zeta_\ell = 0, \quad (28)$$

where

$$\Lambda_\ell(r) = \sqrt{\frac{A}{C}} (\ell + 1). \quad (29)$$

The above equations can be separated to obtain:

$$\frac{\partial^2 \zeta_\ell}{\partial t^2} - \frac{\partial^2 \zeta_\ell}{\partial r_*^2} + V_+(r) \zeta_\ell = 0, \quad (30)$$

and

$$\frac{\partial^2 \chi_\ell}{\partial t^2} - \frac{\partial^2 \chi_\ell}{\partial r_*^2} + V_-(r) \chi_\ell = 0, \quad (31)$$

where:

$$V_\pm = \pm \frac{d\Lambda_\ell}{dr_*} + \Lambda_\ell^2. \quad (32)$$

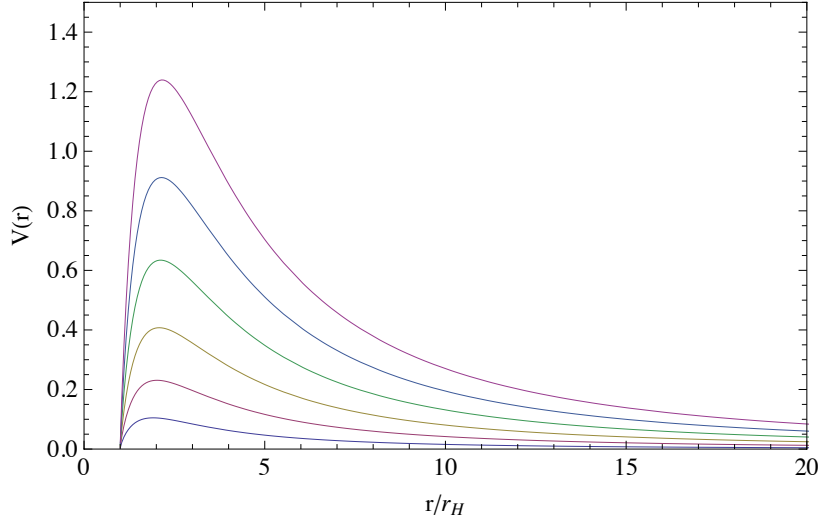


Figure 1. Potential $V(r)$ for Dirac perturbations with $\ell = 0$ (bottom) to $\ell = 5$ (top).

The above equations gives the temporal evolution of Dirac perturbations outside the black hole spacetime [18]. As the potentials V_+ and V_- are supersymmetric to each other in the sense considered by Chandrasekhar in [19], then $\zeta_\ell(t, r)$ and $\chi_\ell(t, r)$ will have similar time evolutions and then they will have the same spectra, both for scattering and quasi-normal. At this point it should be stressed that for the spinor $\tilde{\varphi}_\ell^{(-)}$, we have these two potentials again. In the following we will work with equation (30) and we eliminate the subscript (+) for the effective potential, defining $V(r) \equiv V_+(r)$.

Now for (3+1)-string theory black holes with line element (1), making the identifications $A(r) = f^{-1/2} (1 - \frac{r_H}{r})$, $B(r) = f^{1/2} (1 - \frac{r_H}{r})^{-1}$ and $C(r) = r^2 f^{1/2}$, we can calculate $V(r)$ using (32) with Λ_ℓ given by:

$$\Lambda_\ell = \frac{f^{-1/2}}{r} \sqrt{1 - \frac{r_H}{r}} (\ell + 1). \quad (33)$$

In Figure (1) we show the effective potential for massless Dirac perturbations in four dimensional stringy black holes for various multipole numbers ℓ . In this Figure distances are measured in units of the black hole horizon radius r_H . We see that $V(r)$ has the form of a definite positive potential barrier, i.e, it is a well behaved function that goes to zero at spatial infinity and gets a maximum value at a well defined peak near the event horizon. Then we can expect that the stringy black holes are stable under massless Dirac perturbations, a fact supported by the numerical results that we will present in the next section.

IV. TIME EVOLUTION OF DIRAC PERTURBATIONS

In order to integrate the equation (30) numerically we use the technique developed by Gundlach, Price and Pullin [20]. The first step is to rewrite the wave-like equation (30) in

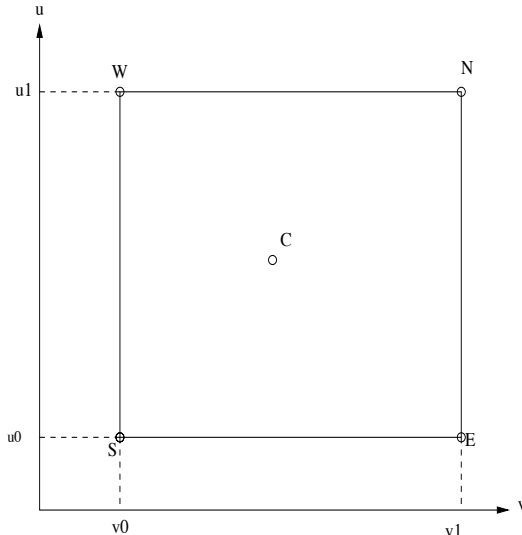


Figure 2. A cell of the integration grid in the plane (u, v) limited by the points N, S, E, W e C . This cell represents an integration step, and the initial data are specified on the left and bottom sides of the rhombus.

terms light-cone coordinates $du = dt - dr_*$ and $dv = dt + dr_*$

$$\left(4 \frac{\partial^2}{\partial u \partial v} + V(u, v)\right) \zeta_\ell(u, v) = 0. \quad (34)$$

and use the following discretized version of the above equation

$$\zeta_\ell(N) = \zeta_\ell(W) + \zeta_\ell(E) - \zeta_\ell(S) - \frac{\Delta u \Delta v}{8} V(S) (\zeta_\ell(W) + \zeta_\ell(E)) + \mathcal{O}(h^4), \quad (35)$$

where the letters S, W, E, N are used to mark the points that limits a particular integration cell of the the grid according to: $S = (u, v)$, $W = (u + \Delta u, v)$, $E = (u, v + \Delta v)$, $N = (u + \Delta u, v + \Delta v)$. In figure 2 we show the cell of a given integration step. We see that the field value at point N depends only of the field values at the points S, E and W . Given a set of initial conditions at the two null surfaces $u = u_0$ and $v = v_0$, we can find, using (35), the value of the field ζ_ℓ inside the rhombus which is built on this two null surfaces. Then,

by iteration of the integration cell, we find the complete data describing the evolution of the fields with time.

The obtained results from the integration in the case of massless Dirac fields in stringy black hole background can be observed as the time-domain profile showed in figures (3) to (7). In such profiles $r = 3r_H$ and the time is measured in units of black hole event horizon.

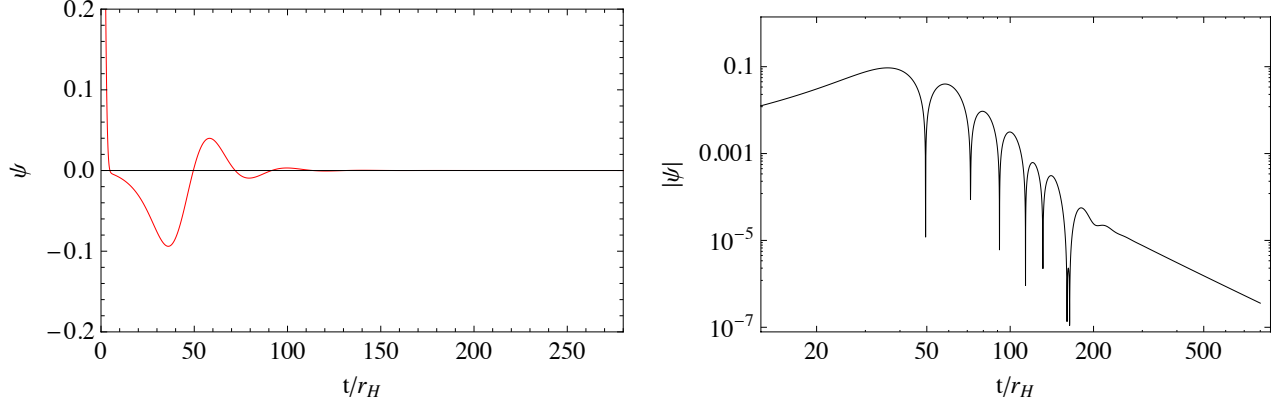


Figure 3. Normal (left) and logarithmic (right) plots of the time-domain evolution of $\ell = 0$ massless Dirac perturbations.

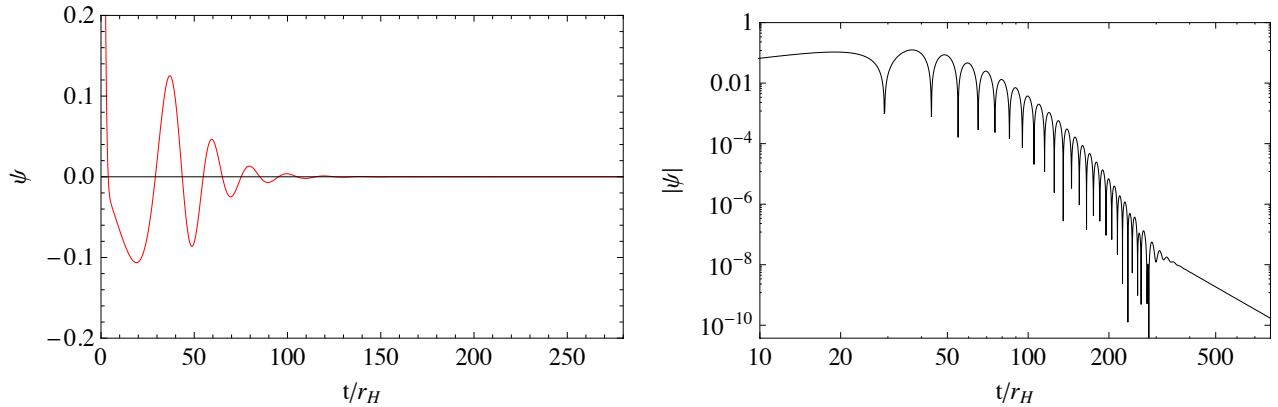


Figure 4. Normal (left) and logarithmic (right) plots of the time-domain evolution of $\ell = 1$ massless Dirac perturbations.

As we can see, the temporal evolution of Dirac perturbations follows the usual dynamics for fields in black holes spacetimes. After a first transient stage strongly dependent on the

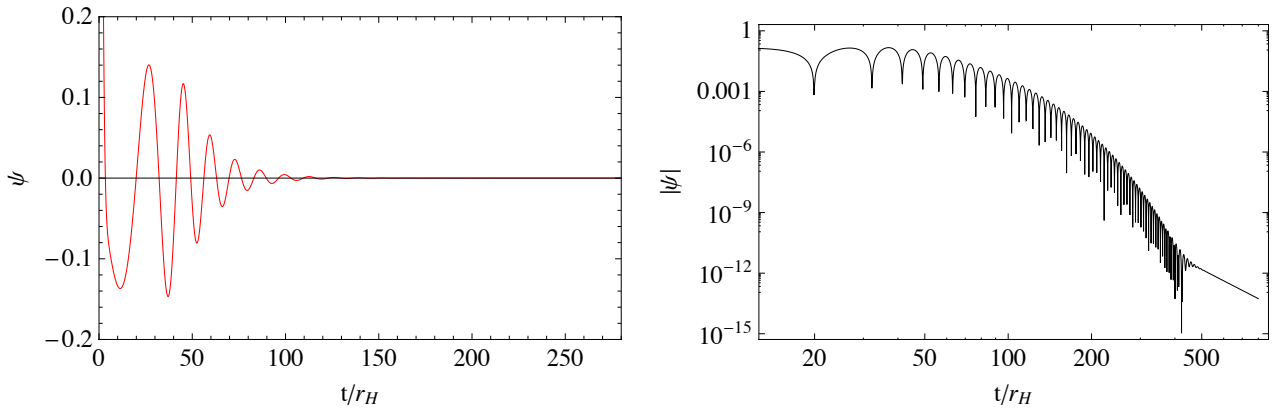


Figure 5. *Normal (left) and logarithmic (right) plots of the time-domain evolution of $\ell = 2$ massless Dirac perturbations.*

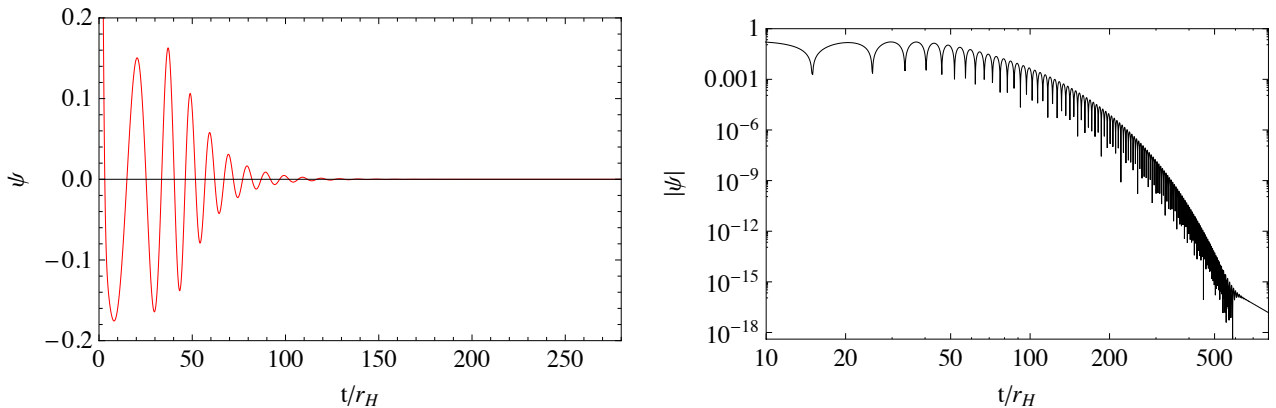


Figure 6. *Normal (left) and logarithmic (right) plots of the time-domain evolution of $\ell = 3$ massless Dirac perturbations.*

initial conditions and the point where the wave profile is observed, we see the characteristic exponential damping of the perturbations called quasinormal ringing, followed by a so-called power law tails at asymptotically late times.

It is important to mention that we perform an extensive numerical exploration of the perturbative dynamics for different values of angular number ℓ , and we have not found any instability for massless Dirac perturbations in four dimensional stringy black holes. It is an expected result due to the positive definite character of the effective potential, as we mentioned in the previous section.

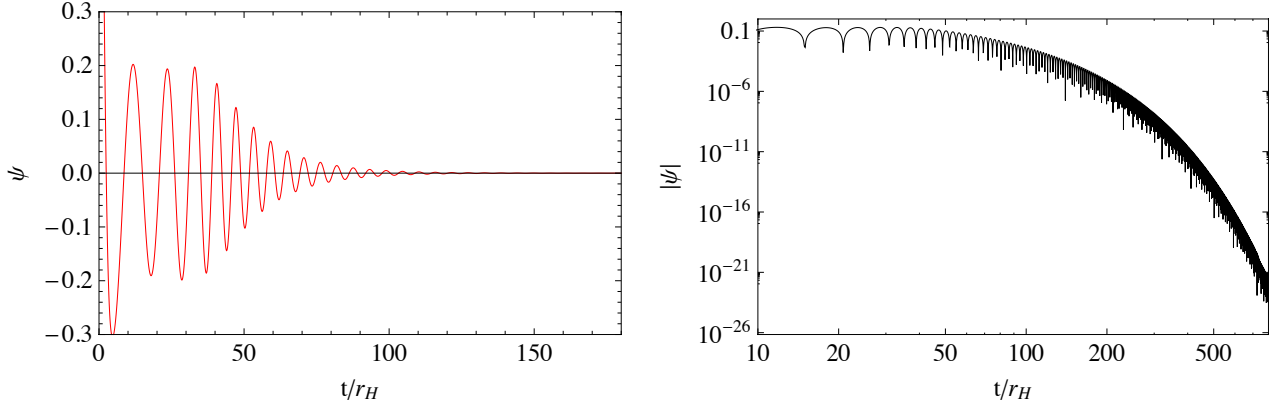


Figure 7. *Normal (left) and logarithmic (right) plots of the time-domain evolution of $\ell = 6$ massless Dirac perturbations.*

V. QNMS USING SIXTH ORDER WKB METHOD AND PRONY FITTING OF CHARACTERISTIC DATA

In the following we will assume for the function $\zeta_\ell(t, r)$ the time dependence:

$$\zeta_\ell(t, r) = Z_\ell(r) \exp(-i\omega_\ell t), \quad (36)$$

Then, the function $Z_\ell(r)$ satisfy the Schrodinger-type equation:

$$\frac{d^2 Z_\ell}{dr_*^2} + [\omega^2 - V(r)] Z_\ell(r) = 0. \quad (37)$$

The quasinormal modes are solutions of the wave equation (30) with the specific boundary conditions requiring pure out-going waves at spatial infinity and pure in-coming waves on the event horizon. Thus no waves come from infinity or the event horizon.

In order to evaluate the quasinormal modes we used two different methods. The first is a semianalytical method to solve equation (37) with the required boundary conditions, based in a WKB-type approximation, that can give accurate values of the lowest (that is longer lived) quasinormal frequencies, and was used in several papers for the determination of quasinormal frequencies in a variety of systems [7, 18, 21–25].

The WKB technique was applied up to first order to finding quasinormal modes for the first time by Shutz and Will [21]. Latter this approach was extended to the third order beyond the eikonal approximation by Iyer and Will [22] and to the sixth order by Konoplya

ℓ	n	Sixth order WKB	Prony
0	0	$0.1527 - 0.0623i$	$0.1525 - 0.0620i$
1	0	$0,3147 - 0.0628i$	$0,3147 - 0.0626i$
2	0	$0.4744 - 0.0629i$	$0.4744 - 0.0629i$
2	1	$0.4663 - 0.1899i$	$0.4661 - 0.1896i$
3	0	$0.6337 - 0.0629i$	$0.6337 - 0.0629i$
3	1	$0.6275 - 0.1894i$	$0.6271 - 0.1880i$
3	2	$0.6156 - 0.3180i$	–
4	0	$0.7928 - 0.0629i$	$0.7928 - 0.0629i$
4	1	$0.7878 - 0.1892i$	$0.7878 - 0.1892i$
4	2	$0.7781 - 0.3169i$	–
4	3	$0.7641 - 0.4466i$	–
5	0	$0.9518 - 0.0629i$	$0.9518 - 0.0629i$
5	1	$0.9476 - 0.1891i$	$0.9476 - 0.1891i$
5	2	$0.9394 - 0.3162i$	–
5	3	$0.9275 - 0.4448i$	–
5	4	$0.9121 - 0.5755i$	–

Table I. Dirac quasinormal frequencies ω_{r_H} for $\ell = 0$ to $\ell = 5$.

[23, 24]. We use in our numerical calculation of quasinormal modes this sixth order WKB expansion. The sixth order WKB expansion gives a relative error which is about two orders less than the third WKB order, and allows us to determine the quasinormal frequencies through the formula

$$i \frac{(\omega^2 - V_0)}{\sqrt{-2V_0''}} - \sum_{j=2}^6 \Pi_j = n + \frac{1}{2}, \quad (38)$$

where $n = 0, 1, 2, \dots$ if $Re(\omega) > 0$ or $n = -1, -2, -3, \dots$ if $Re(\omega) < 0$ is the overtone number. In (38) V_0 is the value of the potential at its maximum as a function of the tortoise coordinate, and V_0'' represents the second derivative of the potential with respect to the tortoise coordinate at its peak. The correction terms Π_j depend on the value of the effective potential and its derivatives (up to the 2i-th order) in the maximum, see [27] and references

ℓ	n	Sixth order WKB	Prony
6	0	$1.1107 - 0.0629i$	$1.1108 - 0.0629i$
6	1	$1.1071 - 0.1890i$	$1.1071 - 0.1890i$
6	2	$1.100 - 0.3158i$	–
6	3	$1.0897 - 0.4437i$	–
6	4	$1.0762 - 0.5732i$	–
6	5	$1.0600 - 0.7045i$	–
7	0	$1.2696 - 0.0629i$	$1.2697 - 0.0629i$
7	1	$1.2665 - 0.1890$	$1.2665 - 0.1889i$
7	2	$1.2603 - 0.3155i$	–
7	3	$1.2511 - 0.4430i$	–
7	4	$1.2392 - 0.5716i$	–
7	5	$1.2246 - 0.7018i$	–
7	6	$1.2077 - 0.8336i$	–

Table II. *Dirac quasinormal frequencies ωr_H for $\ell = 6$ and $\ell = 7$.*

ℓ	n	Sixth order WKB	Prony
8	0	$1.4285 - 0.0629i$	$1.4287 - 0.0629i$
8	1	$1.4257 - 0.1889i$	$1.4258 - 0.1888i$
8	2	$1.4202 - 0.3154i$	–
8	3	$1.4120 - 0.4425i$	–
8	4	$1.4012 - 0.5706i$	–
8	5	$1.3881 - 0.6999i$	–
8	6	$1.3727 - 0.8305i$	–
8	7	$1.3554 - 0.9628i$	–

Table III. *Dirac quasinormal frequencies ωr_H for $\ell = 8$.*

therein.

The second method that we used to find the quasinormal frequencies was the Prony

ℓ	n	Sixth order WKB	Prony
9	0	$1.5873 - 0.0629i$	$1.5876 - 0.0629i$
9	1	$1.5848 - 0.1889i$	$1.5850 - 0.1888i$
9	2	$1.5798 - 0.3152i$	–
9	3	$1.5724 - 0.4421i$	–
9	4	$1.5627 - 0.5698i$	–
9	5	$1.5507 - 0.6985i$	–
9	6	$1.5367 - 0.8283i$	–
9	7	$1.5207 - 0.9594i$	–
9	8	$1.5030 - 1.0920i$	–

Table IV. *Dirac quasinormal frequencies ωr_H for $\ell = 9$.*

ℓ	n	Sixth order WKB	Prony
10	0	$1.7462 - 0.0629i$	$1.7466 - 0.0629i$
10	1	$1.7439 - 0.1889i$	$1.7442 - 0.1887i$
10	2	$1.7393 - 0.3151i$	–
10	3	$1.7326 - 0.4419i$	–
10	4	$1.7237 - 0.5692i$	–
10	5	$1.7127 - 0.6974i$	–
10	6	$1.6998 - 0.8266i$	–
10	7	$1.6850 - 0.9569i$	–
10	8	$1.6686 - 1.0884i$	–
10	9	$1.6505 - 1.2212i$	–

Table V. *Dirac quasinormal frequencies ωr_H for $\ell = 10$.*

method [26, 27] for fitting the time domain profile data by superposition of damping exponents in the form

$$\psi(t) = \sum_{k=1}^p C_k e^{-i\omega_k t}. \quad (39)$$

Assuming that the quasinormal ringing stage begins at $t = 0$ and ends at $t = Nh$, where

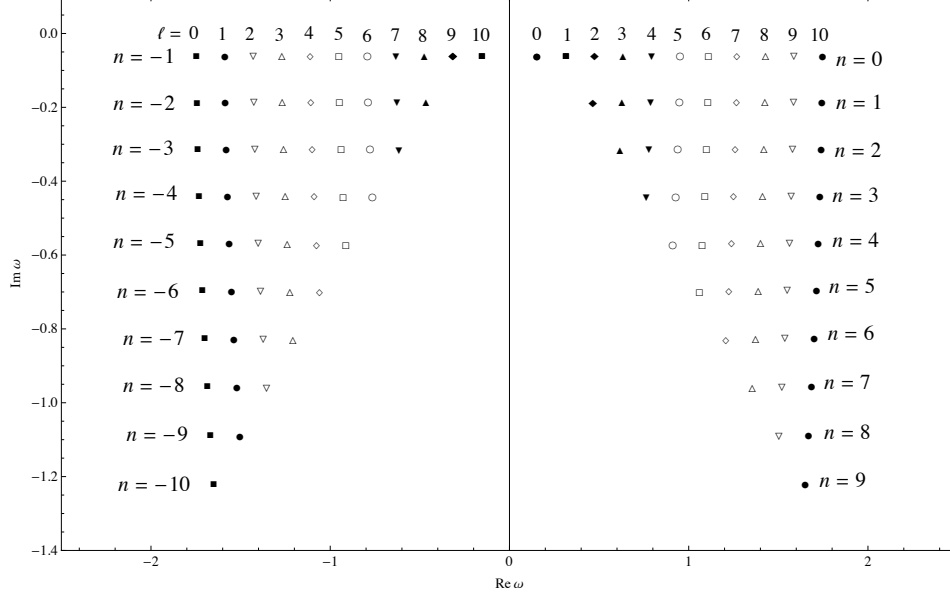


Figure 8. Massless Dirac quasinormal frequencies for various values of l e n .

$N \geq 2p - 1$, then the expression (39) is satisfied for each value in the time profile data

$$x_n \equiv \psi(nh) = \sum_{k=1}^p C_k e^{-i\omega_k n h} = \sum_{k=1}^p C_k z_k^n. \quad (40)$$

From the above expression, we can determine, as we know h , the quasinormal frequencies ω_i once we have determined z_i as functions of x_n . The Prony method allows to find the z_i as roots of the polynomial function $A(z)$ defined as

$$A(z) = \prod_{k=1}^p (z - z_k) = \sum_{m=0}^p \alpha_m z^{p-m}, \quad \alpha_0 = 1. \quad (41)$$

It is possible to show that the unknown coefficients α_m of the polynomial function $A(z)$ satisfy

$$\sum_{m=1}^p \alpha_m x_{n-m} = -x_n. \quad (42)$$

Solving the $N - p + 1 \geq p$ linear equations (42) for α_m we can determine numerically the roots z_a and then the quasinormal frequencies.

It is important to mention the fact that with the Prony method we can obtain very accurate results for the quasinormal frequencies, but the practical application of the method is limited because we need to know with precision the duration of the quasinormal ringing epoch. As this stage is not a precisely defined time interval, in practice, it is difficult to

determine when the quasinormal ringing begins. Therefore, we are able to calculate with high accuracy only two or, sometimes three dominant frequencies.

Tables (I) to (V) shows the results for the quasinormal frequencies measured in units of black hole horizon radius r_H for some values of the multipole moment ℓ . As it is observed, the sixth order WKB approach gives results in good correspondence with that obtained by fitting the numerical integration data using Prony technique.

As usual, the oscillation frequency increase for higher multipole and fixed overtone numbers. The fundamental mode, i.e, that with $\ell = 0$ and $n = 0$ is more long-lived with respect to the other modes, but it is interesting that imaginary part of the $n = 0$ quasinormal frequencies reach very quickly a fixed value for higher multipole numbers.

This situation is different for higher overtone numbers, and the imaginary part for a fixed n increases with ℓ . For $n = 1$ we see that its reach a constant value from the $\ell = 8$, within numerical accuracy. As we expected for stability, all quasinormal frequencies calculated in this work have a well defined negative imaginary part.

VI. LONG TIME TAILS

Another important point to study is the relaxation of the perturbing fermion field outside the black hole. It is a known result that in Schwarzschild black hole neutral massless fields had a late-time behavior for a fixed r dominated by a factor $t^{-(2\ell+3)}$ for each multipole moment ℓ [28, 29].

To study the late-time behavior, we numerically fit the profile data obtained in the appropriate region of the time domain, to extract the power law exponents that describe the relaxation. As a test of our numerical fitting scheme, we obtained the power law exponents for the massless Dirac field considered in this paper in the space-time corresponding to four dimensional Schwarzschild black hole with unit event horizon. As we expected, the results obtained are consistent with the power law falloff mentioned in the previous paragraph.

The case for the late-time fermion decay in (3+1)-stringy black hole is similar, as shows the results of our numerical fitting presented in Figures (9) to (12).

For $\ell = 0$ modes, the numerical decay factor is proportional to $t^{-3.09}$, for $\ell = 1$ is proportional to $t^{-5.03}$. From the results displayed in Figures (9) to (12), and the other obtained fitting the time domain data for all the values of angular numbers considered

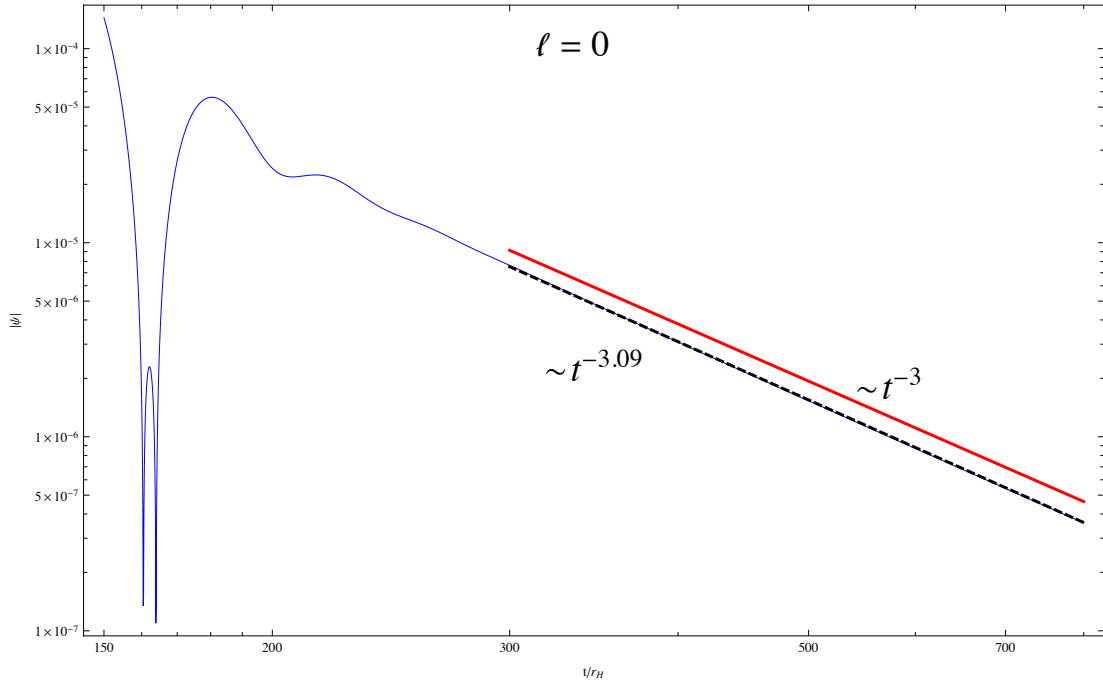


Figure 9. Tail for $\ell = 0$. The power-law coefficients were estimated from numerical data represented in the dotted line. The full red line is the possible analytical result.

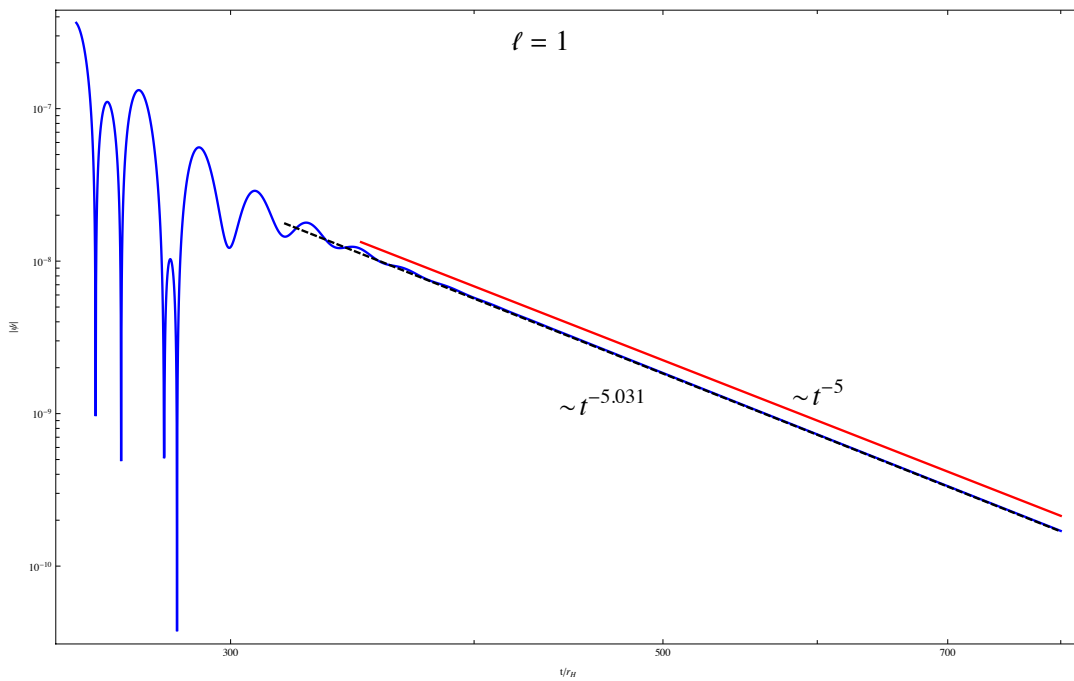


Figure 10. Tail for $\ell = 1$. The power-law coefficients were estimated from numerical data represented in the dotted line. The full red line is the possible analytical result .

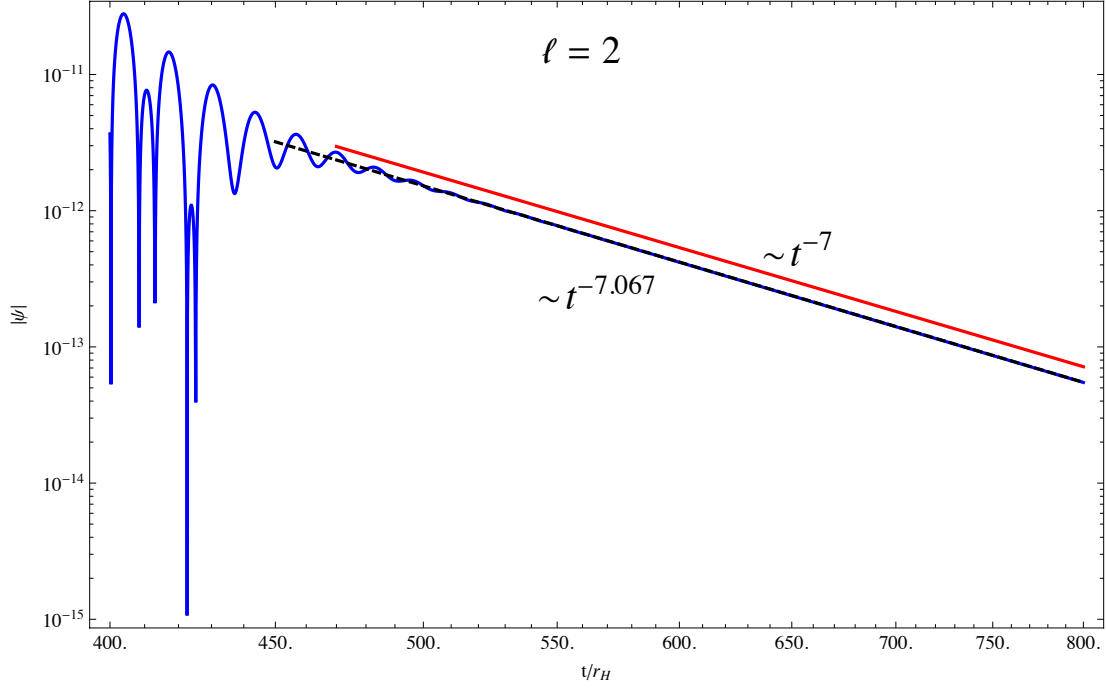


Figure 11. Tail for $\ell = 2$. The power-law coefficients were estimated from numerical data represented in the dotted line. The full red line is the possible analytical result .

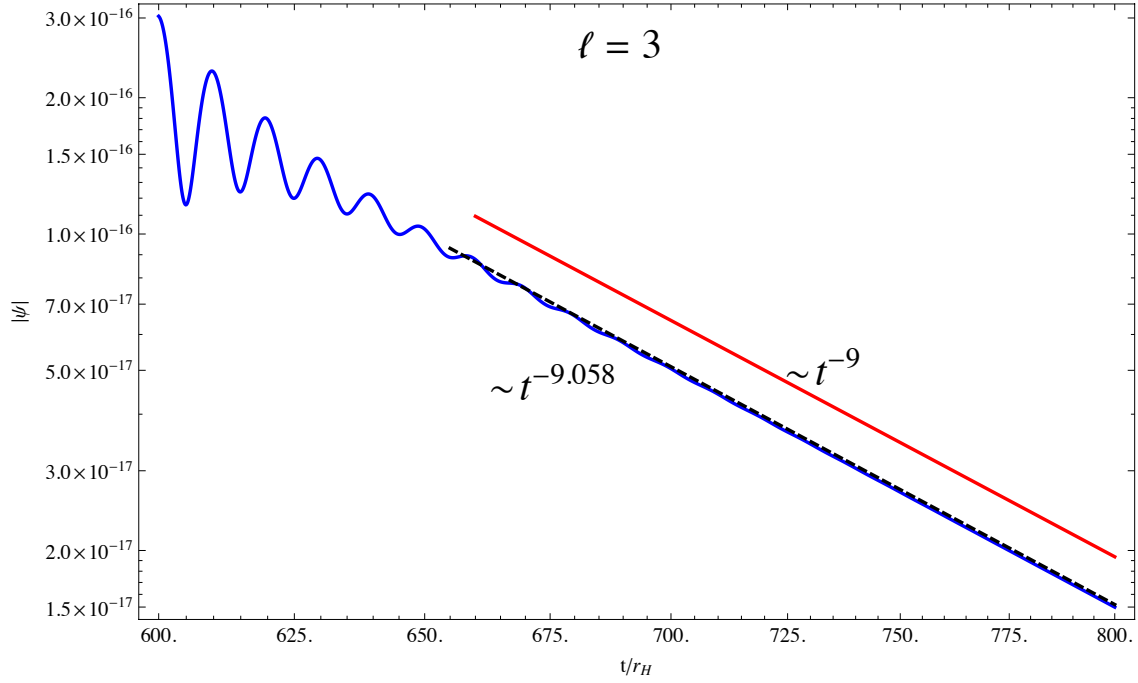


Figure 12. Tail for $\ell = 3$. The power-law coefficients were estimated from numerical data represented in the dotted line. The full red line is the possible analytical result .

in our numerical work, we can determine the power law factor that dominates the falloff of the Dirac field at very late times, in the space-time of the stringy black hole. If we suppose that the decay in the Dirac case is governed by factors of the form $t^{-(\alpha+\beta)}$ for each multipole moment ℓ , then using our numerical results we obtain a decay factor for the Dirac perturbations at late times, that is of the form $t^{-(2\ell+3)}$. We remark at this point that this dependence is only a result consistent with our numerical data for all values of the multipole moments studied, and remains an open problem to obtain this directly from analytical calculations. Then, we can conclude that, outside four dimensional stringy black holes, as well as Schwarzschild black hole, the massless Dirac field shows identical decay at late times.

VII. LARGE ANGULAR MOMENTUM

Although in general the calculation of quasinormal frequencies is performed through numerical tools, we can use the WKB formula to get an analytic expression for the frequencies in the limit of large angular momentum ℓ . It can be obtained expanding the effective potential in terms of small values of $1/\ell$ and using the lowest order of WKB approximation. In the following we suppose for simplicity $Q_i = Q$. So, we get

$$\omega^2 = \ell^2 \sigma(r_m) - i(n + \frac{1}{2}) \sqrt{-2 \frac{d^2 \sigma(r_m)}{dr^2}}, \quad (43)$$

where

$$\sigma(r) = \left(1 - \frac{r_H}{r}\right) \left(1 + \frac{r_H Q}{r}\right)^{-4},$$

and r_m is where the peak of $V(r)$ occurs, and its given by

$$r_m = \frac{r_H}{2} \left\{ \left(Q + \frac{3}{2}\right) + \left[\left(Q + \frac{3}{2}\right)^2 - 2Q \right]^{\frac{1}{2}} \right\}.$$

The quasinormal frequencies calculated using the above expression completely agree with those ones obtained through the six-order WKB approach in the large angular momentum regime. In the table (VI), we can see that the imaginary part of the frequencies for fixed overtone number $n = 0$ goes to a constant value in the limit of large values of ℓ . On the other hand the real part increases as ℓ becomes larger.

ℓ	Dirac quasinormal frequencies
50	$3.96989 - 0.0314673i$
100	$7.93959 - 0.0314681i$
150	$11.9093 - 0.0314682i$
200	$15.8791 - 0.0314683i$

Table VI. *Dirac quasinormal frequencies in the large angular momentum limit with $n = 0$, $r_H = 2$ and $Q = 1$.*

VIII. CONCLUDING REMARKS

We have studied the evolution of massless Dirac perturbations in the space-time of a (3+1)-dimensional black hole solution from string theory. Solving numerically the time evolution equation for this perturbations, we find similar time domain profiles as in the case of Dirac fields in other four dimensional black hole backgrounds. At intermediary times the evolution of fermion perturbations is dominated by quasinormal ringing. We determined the quasinormal frequencies by two different approaches, 6th order WKB and time domain integration with Pronny fitting of the numerical data, obtaining by both methods very close numerical results.

At very late times, the evolution of fermion perturbations in four dimensional stringy black holes shows a power law falloff proportional to $t^{-(2\ell+3)}$, as functions of the multipole number. This behavior is identical to that appeared in the late time evolution of Dirac fields in other four dimensional black holes.

There are extensions of this work that would be considered in the future. In the first place it would be interesting to study of Dirac perturbations in higher dimensional stringy black holes. Another interesting problem is related with the analytical investigation of the late-time behavior of massless Dirac perturbations outside stringy black holes, to obtain a result in correspondence with our numerical estimate for the decay factor. We also find interesting the consideration of the influence of vacuum polarization effects in the quasinormal spectrum for semiclassical stringy black holes. The solutions to some of the above problems will be presented in future reports.

ACKNOWLEDGMENTS

This work has been supported by FAPESP (*Fundação de Amparo à Pesquisa do Estado de São Paulo*) and CNPQ (*Conselho Nacional de Desenvolvimento Científico e Tecnológico*), Brazil. We are grateful to Professor Elcio Abdalla and Dr. Alexander Zhidenko for the useful suggestions and J. Basso Marques for technical support.

-
- [1] J. Polchinski, *String Theory, vols.1,2*, Cambridge University Press, (1998).
 - [2] J. M. Maldacena, arXiv:hep-th/9607235.
 - [3] M. Cvetič and D. Youm, *Phys. Rev. D* **53**, 584 (1996).
 - [4] M. Cvetič and D. Youm, *Nucl. Phys. B* **472**, 249 (1996).
 - [5] M. Cvetič and A. A. Tseytlin, *Nucl. Phys. B* **478**, 181 (1996).
 - [6] G. T. Horowitz, J. M. Maldacena and A. Strominger, *Phys. Lett. B* **383**, 151 (1996).
 - [7] E. Abdalla, O. P. F. Piedra and J. de Oliveira, C. Molina *Phys. Rev. D* **81**, 064001 (2010).
 - [8] T. Regge and J. A. Wheeler, *Phys. Rev.* **108**, 1063 (1957).
 - [9] E. Berti, V. Cardoso and A. O. Starinets, *Class. Quant. Grav.* **26**, 163001 (2009).
 - [10] D. T. Son and A. O. Starinets, *Ann. Rev. Nucl. Part. Sci.* **57**, 95 (2007).
 - [11] S. S. Gubser and A. Karch, *Ann. Rev. Nucl. Part. Sci.* **59**, 145 (2009).
 - [12] S. A. Hartnoll, *Class. Quant. Grav.* **26**, 224002 (2009).
 - [13] G. T. Horowitz, J. M. Maldacena and A. Strominger, *Phys. Lett. B* **383**, 151 (1996).
 - [14] G. W. Gibbons and A. R. Steif, *Phys. Lett. B* **314** 13 (1993).
 - [15] G. Gibbons and M. Rogatko, *Phys. Rev. D* **77**, 044034 (2008).
 - [16] G. Lopez-Ortega, *Lat. Am. J. Phys. Educ.* **3**, 578 (2009).
 - [17] R. Camporesi and A. Higuchi, *J. Geom. Phys.* **20** (1996) 1.
 - [18] H. T. Cho, A. S. Cornell, J. Doukas and W. Naylor *Phys. Rev. D* **75** 104005, (2007)
 - [19] S. Chandrasekar, *The Mathematical theory of Black Holes*, (Clarendon, Oxford, 1983).
 - [20] C. Gundlach, R. H. Price, J. Pullin, *Phys. Rev.* **49**, 883 (1994);
 - [21] B. Shutz and C. M. Will, *Astrophys. J. Lett.* **L33**, 291 (1985).
 - [22] S. Iyer and C. M. Will, *Phys. Rev.* **D35**, 3621 (1987).
 - [23] R. A. Konoplya, *Phys. Rev.* **D68**, 024018 (2003).

- [24] R. A. Konoplya, *J. Phys. Stud.* **8**, 93 (2004).
- [25] R. A. Konoplya and E. Abdalla, *Phys. Rev.* **D71**, 084015 (2005); M.I. Liu, H. I. Liu and Y. X. Gui, *Class. Quantum Grav.* **25**, 105001 (2008); P. Kanti and R. A. Konoplya, *Phys. Rev.* **D73**, 044002 (2006); J. F. Chang, J. Huang and Y. G. Shen *Int. J. Theor. Phys.* **46**, 2617 (2007); J. F. Chang and Y. G. Shen *Int. J. Theor. Phys.* **46**, 1570 (2007); Y. Zhang and Y. X. Gui, *Class. Quantum Grav.* **23**, 6141 (2006); R. A. Konoplya *Phys. Lett.* **B550**, 117 (2002); S. Fernando and K. Arnold, *Gen. Rel. Grav.* **36**, 1805 (2004); H. Kodama, R. A. Konoplya and A. Zhidenko, arXiv:0904.2154; H. Ishihara, M. Kimura, R. A. Konoplya, K. Murata, J. Soda and A. Zhidenko, *Phys. Rev.* **D77**, 084019 (2008); R. A. Konoplya and A. Zhidenko, *Phys. Lett.* **B644**, 186 (2007); R. A. Konoplya, arxiv: 0905.1523; H. Kodama, R. A. Konoplya and A. Zhidenko, arxiv: 0904.2154;
- [26] E. Berti, V. Cardoso, J. A. Gonzales and U. Sperhake , *Phys. Rev.* **D75**, 124017 (2007).
- [27] A. Zhidenko, *PhD Thesis*, arXiv:0903.3555.
- [28] R. H. Price, *Phys. Rev.* **D5**, 2419 (1972).
- [29] R. H. Price and L. M. Burko, *Phys. Rev.* **D70**, 084039 (2004).